3DCP OF ARCHITECTURAL COMPONENTS WITH COMPLEX GEOMETRIES

João Ribeiro
Aires Camões
Paulo J. S. Cruz
Bruno Figueiredo

Driven by the evolution of digital processes in architectural design, the integration of Additive Manufacturing technologies in the production of architectural components has shown significant potential to meet the growing demands for customization and optimization. However, there is still a considerable degree of uncertainty regarding how these techniques can be integrated into current construction systems. Considering that concrete is widely used in the construction industry and that cement production is a significant source of CO_2 emissions, it becomes crucial to explore these new technologies to enhance its efficiency.

To adapt digital fabrication to the specific requirements of real-world context, this study explores the application of 3D Concrete Printing (3DCP) within a prefabrication framework in a controlled laboratory setting. Following the development of the extrusion system, a series of prototypes were produced to systematically scale up manufacturing and identify key process control parameters.

Finally, to demonstrate the applicability of 3DCP in complex environments, this paper presents a case study involving a prototype designed for implementation on a coastal rockfill in Póvoa de Varzim, Portugal. The process begins with a 3D survey of the site, followed by the custom design of a set of discretized platforms composed of medium-sized parts and their corresponding connections. This case study validates the feasibility of the technology and methodology for industrial applications, highlighting its potential for adaptable and efficient construction solutions in challenging contexts.

INTRODUCTION

In recent years, advancements in computational design and digital fabrication – particularly through Additive Manufacturing (AM) – have opened new possibilities for creating complex, free-form, and highly detailed geometries that were previously unattainable with traditional construction methods. Despite clear benefits such as the elimination of formwork, reduction in labour costs, decreased material waste, and the potential for mass customization [1], applications in construction industry remain limited more than two decades after initial experimental trials.

Concrete stands as the most widely utilized material in the construction industry, celebrated for its versatility, mechanical strength, and durability. However, its environmental impact is significant, with cement production alone accounting for approximately 10% of global CO_2 emissions [2]. This high carbon footprint is primarily associated with the calcination of limestone and the energy-intensive processes involved in clinker production [3]. Given these challenges, integrating advanced digital fabrication technologies like 3D Concrete Printing (3DCP) presents a viable pathway to improve material efficiency, reduce waste, and optimize both structural and environmental performance.

By enabling precise material deposition, minimizing the need for formwork, and allowing for topologically optimized geometries, AM techniques have the potential to enhance the economic and ecological sustainability of cementitious materials in construction [4].

Recent research by the Architecture, Construction, and Technology Hub (ACTechHub) at the School of Architecture, Art, and Design at the University of Minho aims to bridge the gap between digital fabrication techniques and practical construction applications. This work contributes to the advancement of 3DCP for scalable and efficient construction solutions. The research explores multiple facets of the technology through the prototyping of various customizable architectural components [5].

Each exploratory research uses computational models, particularly parametric design, to simulate and optimize the AM process and the functional purpose of the components to be produced. This approach, facilitates real-time adjustments of the fabrication parameters, improving the adaptability of AM techniques to varying design requirements. Additionally, it allows for greater design flexibility, enabling the generation of customized complex geometries.

To establish a foundation for this research, a preliminary study was conducted focusing on two critical aspects: the material properties and the extrusion system. It aimed to assess the rheological behaviour of the selected material, ensuring its suitability for the 3DCP process, as well as to refine the printing process by evaluating nozzle design, layer adhesion, deposition accuracy, among other parameters related to robotic 3DCP fabrication. These initial experiments provided valuable insights into the interplay between material composition and printing parameters, informing subsequent stages of component development and fabrication.

Finally, presents an extended project as a proof of concept for the use of 3DCP in a pre-existing complex context, demonstrating rapid prototyping through prefabricated modular solutions and customized, reversible assembly strategies.

A fundamental aspect is the application of Design for Assembly and Disassembly (DfAD) principles. DfAD is a strategic approach that optimizes the construction, maintenance, and deconstruction of structures by ensuring that components can be efficiently assembled and later disassembled without damage. In the context of AM, DfAD principles facilitate modular construction techniques, allowing for the replacement of individual components, minimizing waste, and promoting material circularity [6,7]. By incorporating interlocking geometries, reversible connections, and standardized joint mechanisms, DfAD enhances both structural integrity and adaptability. This approach not only streamlines on-site installation but also supports sustainability by enabling material recovery and reuse, reducing environmental impact, and extending the lifecycle of built systems.

CEMENTITIOUS MIXTURE AND EXTRUSION SYSTEM

As previously stated [8], the application of concrete in AM processes relies on the correct combination of two interrelated elements: material and machine. Given the research context, the study of these aspects followed an experimental approach.

Regarding cementitious mixtures, and based on the empirical knowledge established in reference studies [9; 10] the optimal characteristics for 3D printing are evaluated through four key properties that determine their feasibility: (1) Extrudability, (2) Buildability, (3) Workability, and (4) Open Time. However, the use of cementitious mixtures in AM processes presents inherent conflicts between these required characteristics, for example, material fluidity is essential for pumping and extrusion without blockages, yet excessive fluidity may result in weak printed lines, sagging, or even structural collapse.

The success of a printed element is strongly dependent on the interactions between its raw materials. Based on reference formulations, a series of experiments was conducted to test different cementitious mixtures. The initial compositions consisted of simple mortar mixtures (binder and aggregates with water) and were progressively refined through the addition of various admixtures and additives to enhance their performance until achieving optimal printability. Figure 1 illustrates the composition of a cementitious mixture that successfully met the primary 3D printing requirements.

To address the challenge of maintaining consistent production capacity during extended printing sessions, a set of optimized 3D printing mortar mixes developed by Weber - Saint Gobain (Weber 3D 160-1) and Secil (Secil TEK) were tested. These premixed materials, supplied in 25 kg bags, demonstrated good extrudability and buildability. Weber 3D 160-1 allowed for faster layer deposition, while Secil TEK, with its finer granulometry, resulted in an improved surface finish. In terms of mix preparation, Weber's composition required approximately 11% water by weight, depending on the mixer and extruder used, whereas Secil TEK required around 12.5%. For automated water dosing systems, preliminary tests determined optimal flow rates of 265 L/h for Weber and 305 L/h for Secil.

Based on established models [11], the 3D printing process consists of three interconnected stages: (1) mixture preparation, (2) pumping the material to the extruder nozzle, and (3) depositing the material in layers along a predefined printing path. The initial printing setup at the ARENA Laboratory, illustrated in *Figure 2a,* consisted of three interconnected components: (1) a 120-liter planetary mixer, (2) a mortar pump, and (3) a KUKA KR120 2700-2 industrial robotic arm equipped with a tubular end-effector extrusion tool. The connection between the externally positioned mortar pump

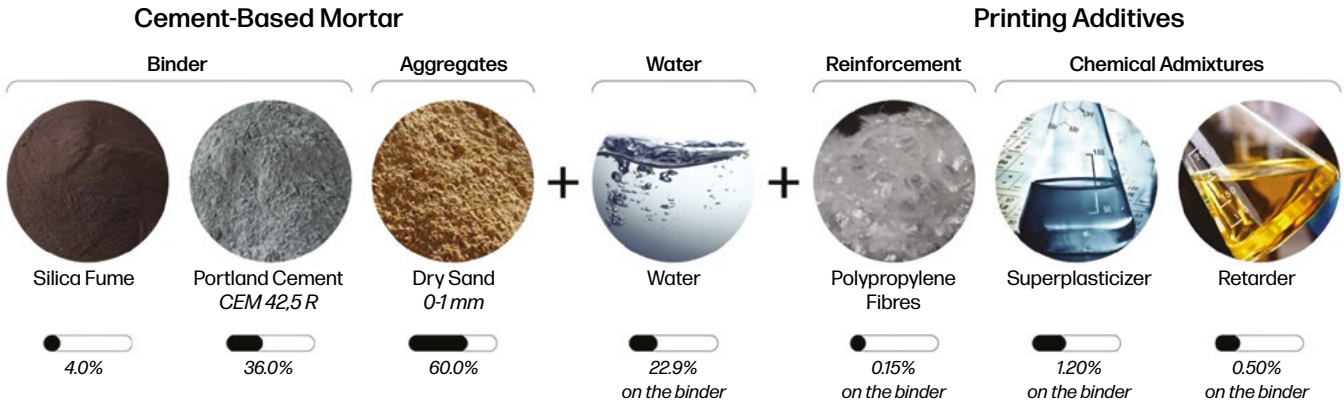

Figure 1: Cementitious mixture recipe.

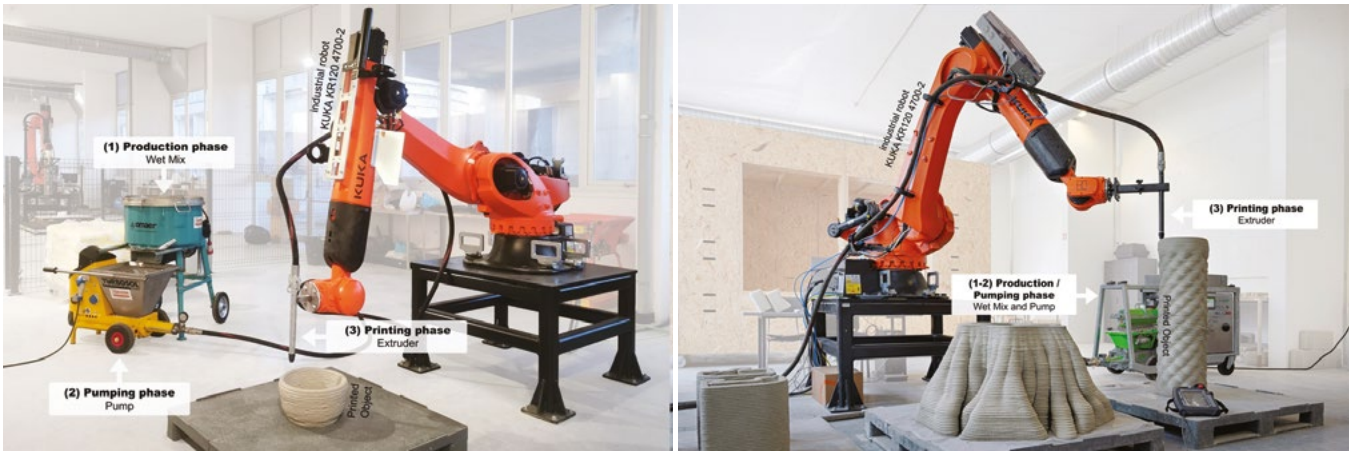

Figure 2: 3DCP printing setups in use at the ARENA laboratory.

and the extrusion tool, mounted on the robotic arm's flange, was achieved through a 25 mm diameter concrete hose.

As shown in *Figure 2b,* this system was later improved by replacing both the planetary mixer (1) and the mortar pump (2) with the MAI Multimix 3D mixing pump, which integrates both mixing and pumping functions into a single unit. Given its continuous horizontal-axis mixing mechanism, the use of pre-packaged dry mixes became essential, allowing precise water dosage adjustments. This solution significantly reduced the workload for operators, as, once correctly configured, the equipment autonomously controlled the entire mixing and pumping process throughout a printing session. Additionally, a modular extrusion tool was developed, incorporating interchangeable extension components that enable greater horizontal and vertical reach of the extruder.

EXPERIMENTAL TESTS

This section outlines a series of preliminary experiments conducted to assess the potential of 3DCP processes. The experimental workflow explored various applications, including structural components, furniture and maritime elements. Through an iterative trial-and-error approach, the main weaknesses of each proposal were identified, and methodologies were developed to overcome their primary constraints. The conclusions drawn from these experiments ultimately informed the definition of the case study.

Mortar tests were carried out using the KUKA KR120 robotic printing setup shown in *Figure 2*. These experiments successfully validated the feasibility of using Weber 3D 160-1 mortar for AM applications, demonstrating its extrudability, buildability, and overall suitability for automated construction. The knowledge gained from these trials was progressively incorporated into subsequent prototype developments. Some of these prototypes will be further detailed in other scientific publications.

Characterization Specimens

A series of extrusion tests were performed using standardized geometries (e.g., straight and inclined cylinders, ovalized specimens with varying curvature degrees, surface filling patterns, etc.) to establish optimal parameters for the extrusion system. These experiments demonstrated that, even with a fixed extruder nozzle (in this case, a 20 mm circular cross-section), substantially different layer geometries could be achieved by adjusting printing parameters. Key variables included layer height, robot speed, pump flow rate, and geometric constraints such as the inclination of extruded walls relative to the base. *Figure 3* presents a set of four printed specimens where only the layer height was varied (20 mm, 15 mm, 10 mm, and 5 mm), revealing significant differences in the final characteristics of the printed elements. Keeping the extrusion speed and flow constant, layer thickness changed.

Conversely, *Figure 4* illustrates the variation in layer height resulting from a different strategy, in which the robot's movement speed was progressively adjusted during the printing process as a function of the different layer heights. By maintaining a constant pump flow rate, this approach ensured that only the necessary amount of material was deposited, thereby preserving a consistent layer thickness of 30 mm throughout the print.

Demonstration cube

A cube was designed to test various surface patterns and textures through direct manipulation of extrusion paths. Each of its four faces features a distinct variation: (a) a zigzag pattern applied every two layers; (b) another zigzag pattern applied alternately on all layers; (c) a wavy surface; and (d) embossed lettering in low relief. By utilizing attraction points to modulate the spacing within the zigzag patterns, the experiment enabled the precise evaluation of optimal spacing for achieving the intended visual and structural effects. Additionally, the feasibility of incorporating an internal M-shaped reinforcement structure without interrupting the extrusion was assessed. The fabrication of the component, illustrated in *Figure 5*, required approximately 40 minutes.

Concrete column

The scale-up of previously tested geometries required a comprehensive review of printing parameters. A hollow column with a wavy pattern was produced to assess the material's structural viability. The prototype had a 35 cm base diameter, a height of 80 centimetres, and an approximate weight of 80 kg. It was manufactured using a 20 mm extruder nozzle, 10 mm layer height, and a robotic movement speed of 100 mm/s, with a total printing time of about 15 minutes. This type of prototype has potential for integration as a lost formwork system in architectural applications.

The column emerged as an alternative approach to a previous AM ceramic experiment for the columns of a porticoed system originally developed as part of the PhD of João Carvalho [12]. In the initial design, each column consisted of twelve ceramic segments, constrained by the limitations of the ceramic 3D printing process, such as the printer's working area, kiln capacity, and material deformation during curing and firing. To address these constraints, a concrete-based variation was developed. Free from the manufacturing restrictions of ceramic printing, the new column design consists of only two printed segments, each 80 cm high only due to the need for manipulation and placement *in situ*.

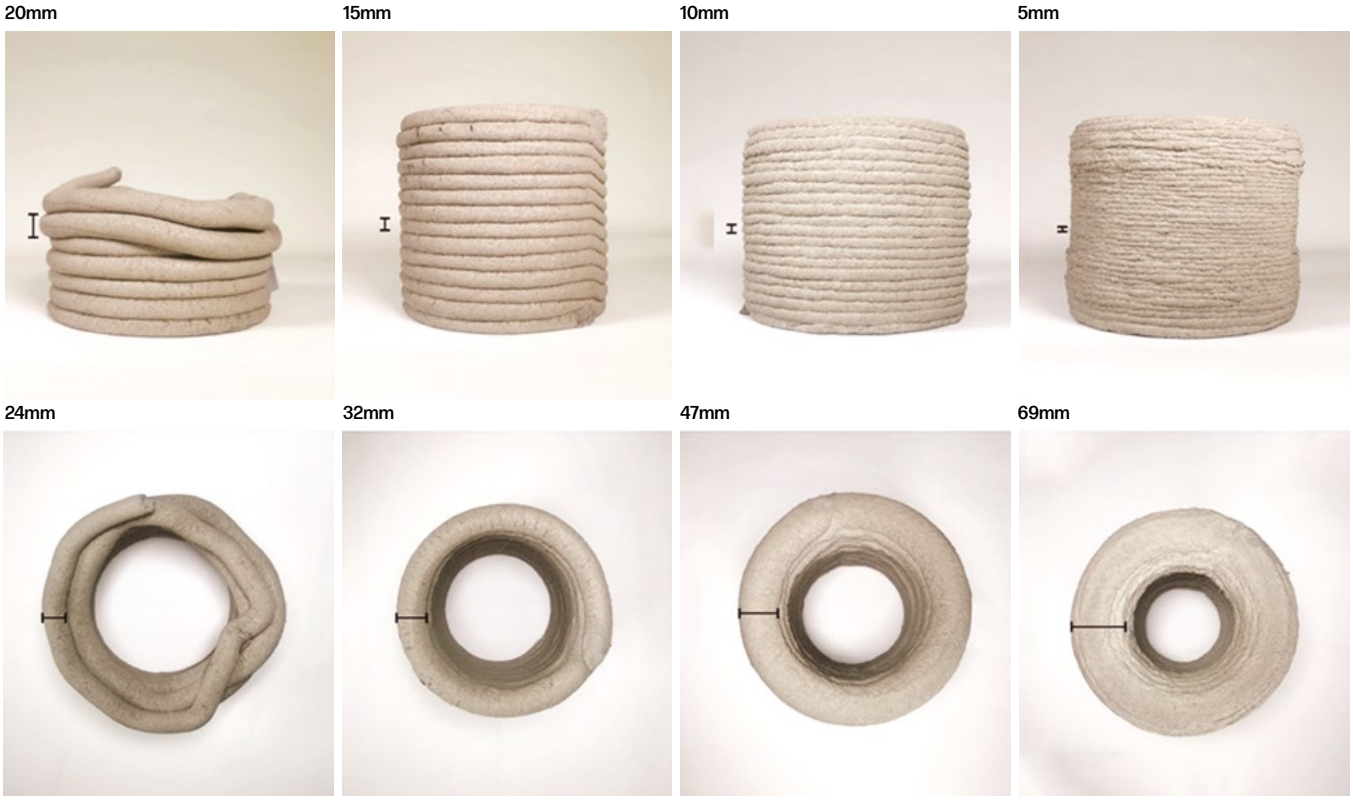

Figure 3: Printed test specimens with varying layer heights.

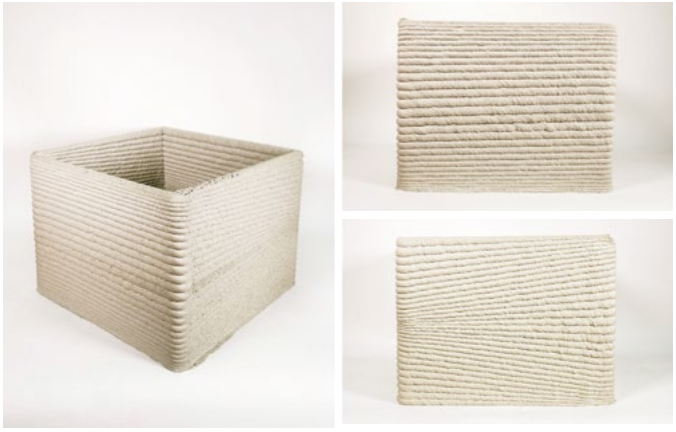

Figure 4: Relationship between printing speed and Amount of material deposited.

Figure 5: Demonstrator prototype with different textures and internal reinforcement.

Figure 6: Comparison between the ceramic column composed of twelve segments and the concrete column composed of two segments.

Figure 7: Interlocking concrete wavy wall.

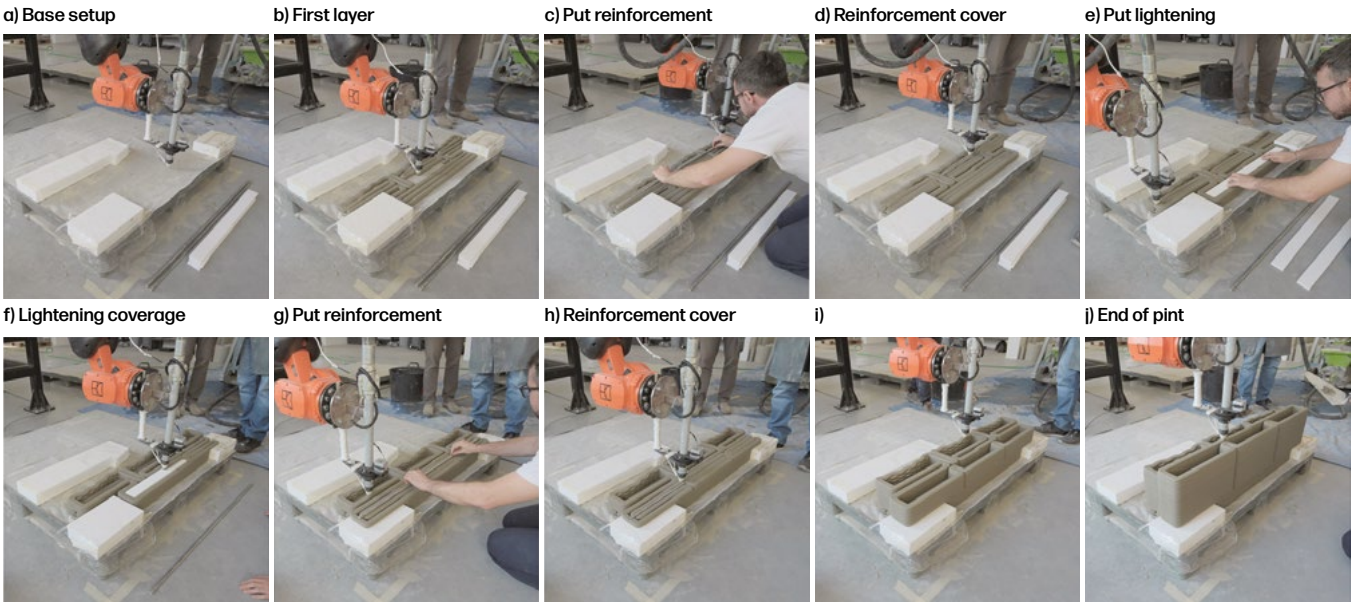

Figure 8: Printing process of a window lintel.

Figure 9: Concrete bench prototype - detail of the seam between layers (left) and full view (right).

Figure 10: Artificial reef prototype printed in ceramic (left) and concrete (right).

Moreover, the concrete column was designed to maintain compatibility with the capital/connection system of the ceramic column with beams. To achieve this, a detailed survey of the ceramic segment geometry was conducted, informing the digital model of the concrete counterpart. The printed segments functioned as integrated formwork for the column. *Figure 6* presents the completed prototype after reinforcement placement and core concreting, alongside the previously developed ceramic column.

Interlocking wavy wall

The concrete wavy wall prototype, shown in *Figure 7*, result from a 3DCP prefabricated masonry system that adheres the following design principles: (1) it consists of a double wall system; (2) stability is mainly ensured by the incorporation of a bidirectional interlocking system into each block, which can be complemented by weak chemical bonds for waterproofing; (3) provides the corrugated surface finish on the exterior; (4) supports the application of an interior wall covering; and (5) it is designed to be lightweight and easily transportable, allowing assembly and disassembly by a single operator.

Beyond exploring the 3DCP process, the prototype aims to achieve a high level of reversibility, aligning with DfAD principles. Additionally, the interconnected internal voids can be utilized for routing infrastructure or for the insertion of insulation materials, enhancing the wall's thermal and acoustic performance.

To address a common limitation of 3D printing – the creation of lintels for windows or doors – ongoing research has focused on integrating reinforcement and light weighting strategies during the printing process. The image below (*Figure 8*) step-by-step illustrates the fabrication of an 80 cm-wide lintel, in which reinforcement bars were embedded in the lower section, while polystyrene inserts were incorporated to reduce weight.

Urban furniture

The design of the concrete bench, developed in collaboration with students Pedro Costa and Ricardo Faria as part of a training course on Robotic Fabrication in Design, Architecture, and Construction, presents a practical application of previously tested concepts. Following a parametric design methodology that allows customization based on desired characteristics, the bench was tailored to accommodate human morphology. The dimensions were constrained by the 1.2 × 1.2 meters printing area, and the piece was designed with a bipartite contour: (1) the lower surface remains regular, while (2) the upper surface features a textile-like texture generated through the zigzag manipulation of extrusion paths. Internally, a reinforcement structure was integrated, connecting both surfaces and providing the necessary support for the waved upper section. During the preparation, the contours and internal reinforcement were fused layer by layer, creating a continuous extrusion path from the first to the last layer. The prototype was printed in a rotational orientation of 90° relative to its final position (*Figure 9*).

Artificial reef

Differential growth algorithms were proposed as design principles to design artificial reefs to be 3DCP manufactured, enhancing marine biodiversity through bioinspired complexity. By leveraging differential growth modelling in Grasshopper 3D, structures were designed with intricate, porous geometries that mimic natural reef formations, providing cavernous pocket spaces for marine species to inhabit, hide, and reproduce [13; 14]. These artificial reef structures align with karst formations and natural reef environments, which have been shown to foster high levels of biodiversity by creating numerous ecological niches for marine organisms [15].

AM techniques have been particularly advantageous in this context for precise fabrication of bioinspired structures using eco-friendly, marine-compatible materials, ensuring long-term stability and integration within the underwater ecosystem [16]. Building upon previous small-scale ceramic artificial reef prototypes as described by C. Lange *et al.* [17], a similar geometry was fabricated in concrete, demonstrating the scalability and structural integrity of AM techniques for marine conservation. The prototype, shown in *Figure 10*, features a hexagonal base measuring one meter in diameter, a height of 50 centimetres, and a total weight of approximately 300 kilograms, making it suitable for deployment in marine conditions. When deployed in marine environments, these porous structures provide essential shelter and protection for various marine species, supporting the natural development of ecosystems in artificial habitats.

ROCKY PONTOON PLATFORM SYSTEM

Coastal and river erosion have emerged as critical challenges for cities located along shorelines worldwide, driven by both human activities – such as the continuous development of coastal areas and rising average sea levels – and natural processes, including wave and tidal action. This phenomenon primarily results from the gradual displacement and transport of coastal sediments due to oceanic forces, such as currents and tides, leading to shoreline retreat and the progressive loss of land to the sea [18].

To mitigate these impacts, engineers have traditionally constructed large-scale structures such as breakwaters and seawalls, composed of natural stone or concrete

elements arranged to effectively dissipate wave energy [19]. These structures often occupy valuable coastal zones – such as beaches, urban waterfronts, or riverbanks – that are also used for recreational and occupational activities, including fishing and walking. Despite their protective role, the irregular shapes and voids within these structures can pose safety risks, and their complex nature makes non-intrusive rehabilitation or enhancement technically challenging.

Nevertheless, significant technological progress has been made in computational design, photogrammetric surveying, and 3D printing techniques [20]. On one hand, advanced digital tools and 3D scanning technologies allow for precise documentation and modelling of complex environments that were once difficult to capture accurately. On the other hand, 3DCP enables the mass production of unique, customizable geometries, streamlining construction processes in highly complex contexts. This approach eliminates the need for bespoke formwork for each individual geometry and allows for the creation of hollow components. When combined with structural and formal optimization algorithms, these innovations can significantly reduce raw material usage, component weight, and the size of required structural elements, while also enabling the internal structure to be tailored to specific functional requirements.

Intervention proposal

Recognizing the limitations of 3D-printed structures in fully replacing the heavy rockfill that constitutes breakwaters and riverbanks, a strategic approach was developed to implement a modular platform system designed specifically for these irregular surfaces. The primary objective of this system is to provide functional versatility, supporting the integration of walkways, recreational areas, fishing spots, sea-view platforms, urban furniture, and other infrastructure elements that promote the safe and accessible use of these environments (*Figure 11*).

The adoption of digital design and advanced manufacturing technologies is driven by the need to respond effectively to the site's inherent geometric complexity. Additionally, the intervention is guided by the principles of DfAD, ensuring that the system remains temporary, reversible, and reusable. This methodology minimizes intrusive or destructive modifications to the existing structures, thereby preserving both their structural integrity and the surrounding environmental context.

To achieve a precise fit with the irregular topography of breakwater rocks, photogrammetry technologies were used to capture detailed digital models of the rock geometries. These high-resolution models guided the development of generative design algorithms, facilitating the creation of platform structures that integrate seamlessly with the site's contours. On the production side, 3DCP was employed to fabricate self-supporting segments that accurately replicate the digital geometries, minimizing the need for mechanical or chemical anchoring.

From an ecological perspective, we argue that AM processes can provide innovative solutions to support local marine biodiversity. This artificial platforms, designed with hollow interiors, feature internal structures that can be optimized to fulfil two key objectives: (1) enhancing the mechanical strength of the components to withstand the dynamic forces of ocean waves; and (2) creating internal cavities with varying textures and dimensions to promote the establishment of native marine life, fostering local biodiversity through the creation of microhabitats and ecological niches conducive to the growth of marine flora and fauna.

Methodology

The development process for this study was structured in key stages, as illustrated in *Figure 12*. The first stage involved conducting a photogrammetric survey of the intervention site. This was followed by the post-processing of the 3D model generated from the survey, allowing for a detailed representation of the site's topography *(Digitization).*

In the third stage, design considerations were addressed using a parametric workflow implemented in Grasshopper. This approach facilitated the generation of design solutions based on predefined manufacturing constraints – such as maximum allowable inclination angles – and additional parameters, including the intended programmatic functions and the overall architectural concept (*Form generation).*

The subsequent two stages focused on fabrication. Initially, in the fourth stage, print path generation was carried out for each individual platform, incorporating the design of internal structural elements. This was followed by the production phase, conducted in a controlled laboratory environment using a 3DCP extrusion system mediated by a robotic arm *(Fabrication process).*

Finally, the prefabricated components would be transported to the intervention site, where in-situ post-tensioning would be performed to achieve the final structural assembly. This step has been replaced by laboratory testing *(Laboratory assembly).*

Implementation

The prototype production process began with the selection of the intervention site. After comparing several urban waterfront areas, the study identified the Breakwater of the Póvoa de Varzim Lighthouse (Oporto, Portugal) as the chosen case study. The specific intervention area within this site was chosen based on observed fishing activities, the rugged topography, and the safety hazards associated with accessing the area (elevation difference). *Figure 13* highlights the selected location.

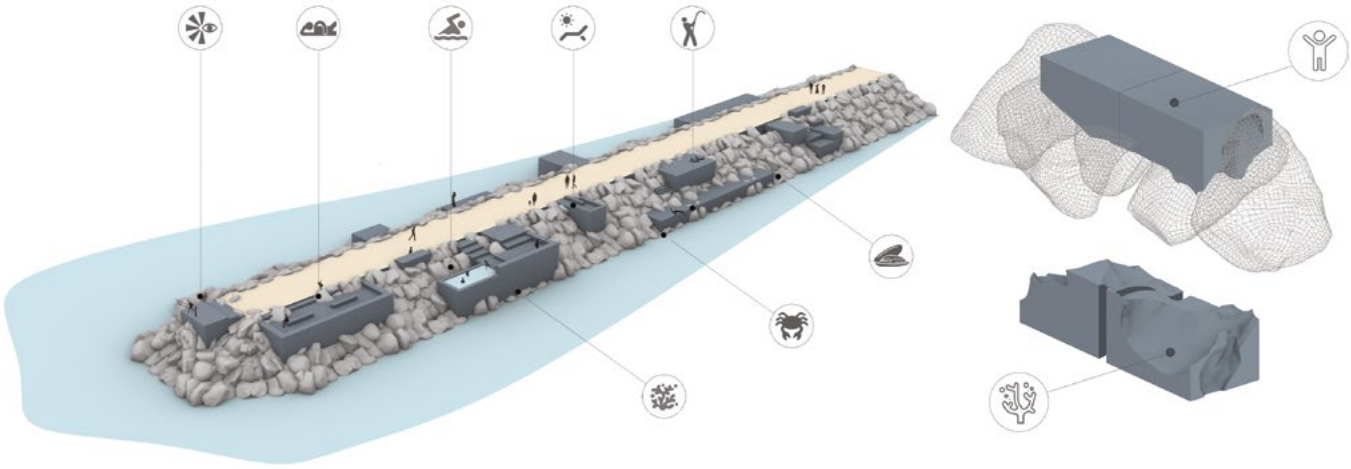

Figure 11: Occupation scheme of rocky breakwaters, with custom-made precast 3DCP components.

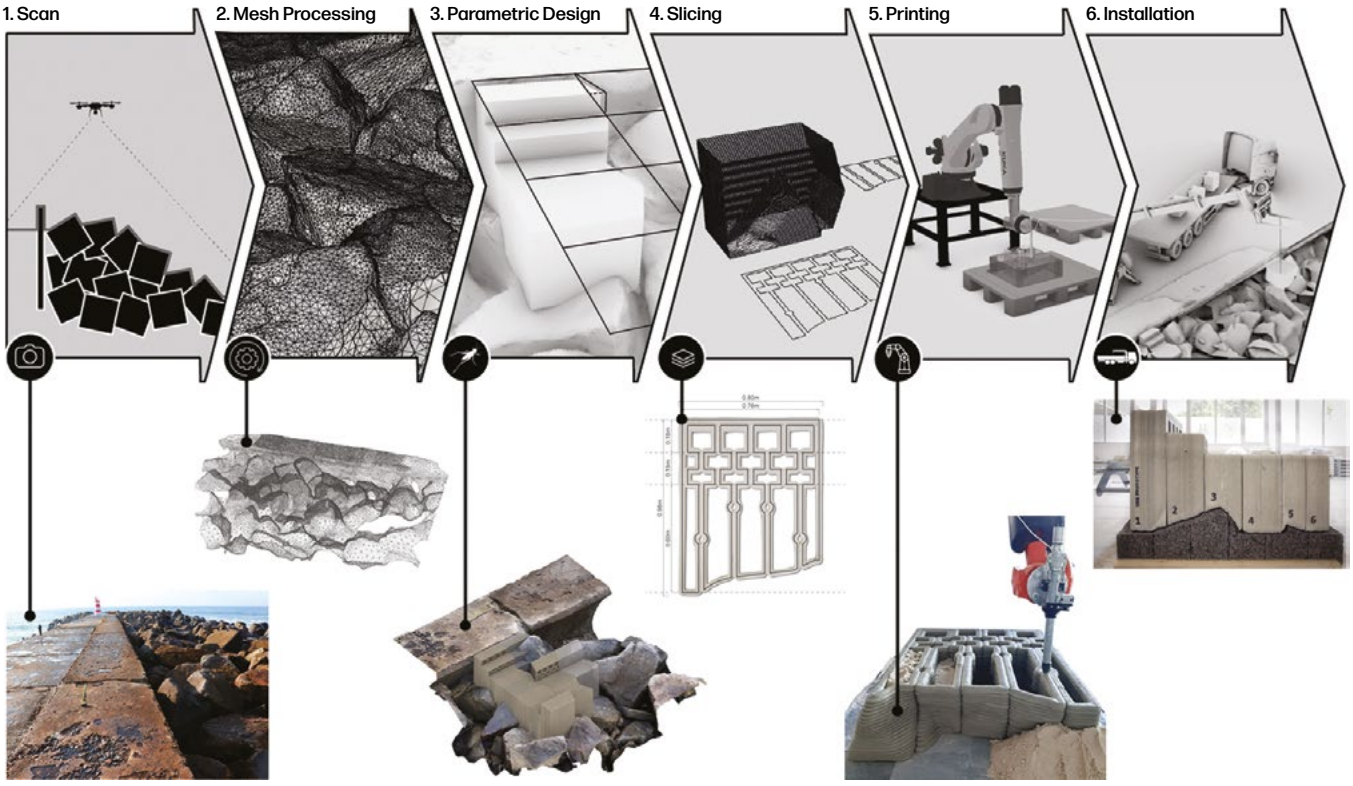

Figure 12: Scheme of the working methodology.

Digitization

Photogrammetry was chosen for 3D surveying of the breakwater area due to its high resolution, suitability for outdoor environments, and cost-effectiveness. The survey was conducted by a single operator using a mid-range digital camera, capturing approximately 120 photographs. Each image was taken while moving around the selected area of interest in circular paths, varying both the distance from the rocks and the camera angle to minimize blind spots and avoiding factors such as self-shadowing or reflections that could affect the quality of the mesh construction *(Figure 14a).*

After testing various photogrammetry software, *PhotoCatch* provided the fastest and highest-quality reconstruction, processing 3.5 m² in about 30 minutes. The resulting mesh was then imported into *MeshLab* for post-processing, where the *quadratic-edge collapse* algorithm reduced the mesh size by 40%, while maintaining a deviation of less than 1 cm. This reduction proved essential to optimizing the efficiency of subsequent design phases, ensuring that the necessary geometric accuracy was preserved for precise, site-specific fabrication (*Figure 14b*).

Form generation

The geometric definition process for each slab was developed through a parametric workflow that can be adapted to any section of the breakwater. This system begins by delineating an area of interest, onto which a rationalized grid is superimposed, with each cell representing a discrete module of the platform. Various topological grid configurations were analysed to identify the optimal arrangement that balances local support, effective interlocking behaviour, and geometric suitability for 3DCP fabrication.

Figure 15 illustrates the generative scheme of the platform design. Using the 3D model obtained through the digitalization (a), the process began with the establishment of a rationalized grid with 80 × 80 cm cells over the area of interest (b). Then, a genetic algorithm was employed to adjust the placement of the grid cells, optimizing their location to maximize contact with the underlying rock formations. The module positions were fixed to ensure each unit maintains an adequate load distribution (c). To enhance structural interlocking between adjacent modules, the vertical edges were modified by introducing mid-point offsets, creating a zigzag pattern that promotes mechanical interlocking (d). Subsequently, further subdivision was applied to limit surface inclinations, ensuring that all components meet the manufacturability constraints of the 3DCP process (e). This approach resulted in modules of varying heights (20 cm and 30 cm), all within the dimensional and structural limits of the printing equipment and with a manageable weight to allow the transportation.

The generated grid defines the upper perimeter of each slab. To derive the volumetric configuration, a point cloud was created (f) and projected along the z-axis onto the 3D mesh of the site survey, populating the area of each module (g). A *Delaunay triangulation* algorithm was then applied to generate a mesh for each slab, followed by a quadratic reconstruction of the meshes faces to correct surface imperfections (h). Finally, the mesh was extruded to achieve the desired height, corresponding to the functional role of each module within the platform (i). This method was preferred over direct Boolean operations between the extruded geometry and the terrain mesh to avoid potential issues during print preparation.

Each slab's geometry is unique, shaped by four key criteria: (1) it conforms precisely to the geometry of the supporting rocks, ensuring a secure fit; (2) it interlocks seamlessly with neighbouring modules through custom-designed joints; (3) it fulfils specific programmatic functions on the surface, such as circulation pathways and resting areas; and (4) it contributes to local biodiversity by incorporating internal cavities that create new habitats for marine species. *Figure 16* presents a 3D simulation of part of the platform to be produced.

Fabrication process

The fabrication of the prototype required a preparatory phase in which the 3D models of each component were translated into a set of toolpaths guiding the robotic extrusion process. In polymer-based AM, slicing software typically automates this step, however, concrete printing introduces additional challenges that necessitate a more controlled approach. Given that the contact geometry with the breakwater rocks was unique for each piece, a custom script was developed in Grasshopper to assist in generating the extrusion paths. Additionally, the optimal printing orientation of the components was analysed. Preliminary tests determined that printing the elements in a lateral position, rotated 90° from their final in-situ placement, would yield the best structural performance and minimize deformations.

The generation of contour curves for each platform component followed a three-step process. First, a series of horizontal planes were defined, spaced according to the layer height, which was set at 10 mm. Next, the intersections between these planes and the 3D model of each component were computed, resulting in a sequence of closed curves outlining the external boundaries. Finally, these curves were offset by half the extrusion width (approximately 35 – 40 mm for a 20 mm nozzle) to ensure a continuous and stable printing path. After analysing the generated toolpaths, the base orientation of each piece was defined to reduce deformations caused by inadequate support for upper layers.

The next step involved designing the internal structure of each component. A parametric approach was

adopted to accommodate different functional requirements, including staircases, circulation areas and seating elements, while ensuring sufficient internal support for the upper layers. The internal structure followed a cellular pattern with three primary objectives: (1) enhancing the structural resistance of the printed element, (2) creating voids that facilitate wave energy dissipation, and (3) incorporating morphological features with textures and concavities to promote the attachment of native marine flora and fauna. This proposal resulted in a design of an internal alveolar structure that can be freely adjusted, ensuring the necessary continuities between the elements.

Figure 17 illustrates three distinct types of cross-section that configure the platform access ladder. For instance, the leftmost section features four cells of varying heights. Their alveolar boundaries are aligned horizontally to ensure adequate support for upper layers. Additionally, duplicated vertical lines were incorporated to enhance the component's overall strength and provide a continuous printing path with well-aligned layer seams.

Finally, a connection system was integrated to enable modular assembly and disassembly. To maintain structural flexibility and allow for reversibility, chemical bonding between elements was avoided. Instead, post-tensioning systems with steel cables were used during assembly. To accommodate this approach, voids were strategically placed within the printed modules to allow for cable passage. These cables were arranged perpendicularly to the printed layers and tensioned to apply compressive forces, effectively unifying the platform and reducing tensile stresses. *Figure 18* illustrates the modular components and simulates the assembly process.

Based on prior calibration, the optimal printing parameters included a layer height of 10 mm, a 20 mm extrusion nozzle and a printing speed of 100 mm/s. The pump pressure was adjusted to maintain a consistent extrusion width of approximately 40 mm throughout the process. *Figure 19* illustrates the printing of one of the parts, using sand as support material for the steeper surfaces.

Laboratory assembly

Since on-site positioning was not permitted, a laboratory-based validation of the concept was conducted by replicating the geometry of the digitized rocks. This artificial topography was created through a milling process using a series of black agglomerated cork blocks (each measuring 1000 × 500 × 320 mm), shaped with the assistance of a robotic arm equipped with an industrial spindle. *Figure 20* illustrates this process.

The milling procedure was carried out in two stages: (1) Initially, a rough cut was performed using a terraced approach, with cutting paths generated in Fusion 360 and subsequently imported into Grasshopper for KRL code generation. This process, which took approximately 12 hours, was executed using a 12 mm flat-end mill, with an 8 mm stepover and a 20 mm stepdown; (2) The final finishing stage was then applied. In this phase, a 12 mm ball-nose end mill was used, following parallel toolpaths spaced 6 mm apart in both orthogonal directions of the surface. These toolpaths were directly generated in Grasshopper by interpolating surface points with a 20 mm offset. To enhance the surface quality, the tool orientation was determined by the normal vector of the surface at each interpolated point. *Figure 21* presents the fully refined cork base.

The final stage involved positioning the six printed components onto the previously milled cork base. Given that each printed component weighed between 150 and 300 kg, depending on its size, their transport and placement required the use of a forklift or a crane system. A rubber strip was inserted between each adjoining module to absorb potential irregularities and prevent direct contact between elements. Once all components were positioned, steel cables were passed through the designated conduits and tensioned using a torque wrench. *Figure 22* depicts the completed prototype.

CONCLUSION

This research demonstrates the versatility and efficiency of 3DCP, emphasizing its potential to respond in complex real-world context. By integrating advanced digital fabrication techniques with prefabrication logic, the study highlights the adaptability of cementitious AM to diverse applications, from architectural systems to coastal infrastructure solutions.

For instance, the production of C*oncrete column* prototype, showcases key advantages in terms of efficiency, sustainability, and adaptability. In addition to being able to obtain geometries that are impossible to achieve with traditional methodologies, the use of this technology to produce the integrated column formwork reduces material waste and the labour required. Furthermore, the concrete column maintains the topologically optimized geometry of the ceramic column, yet produces it in a 95% faster printing time. Adding to this the need for curing and firing the ceramic material, we conclude that we have achieved a significantly improving construction speed, reducing the time gap between production and on-site assembly.

The *Rocky pontoon platform system*, highlights the potential of 3DCP in coastal environments, demonstrating the feasibility of digitally fabricated solutions for adapting to complex terrains. Key advantages include the elimination of formwork, a 42% weight reduction through strategically placed voids that enhance transportability and installation feasibility, and custom-fit fabrication using

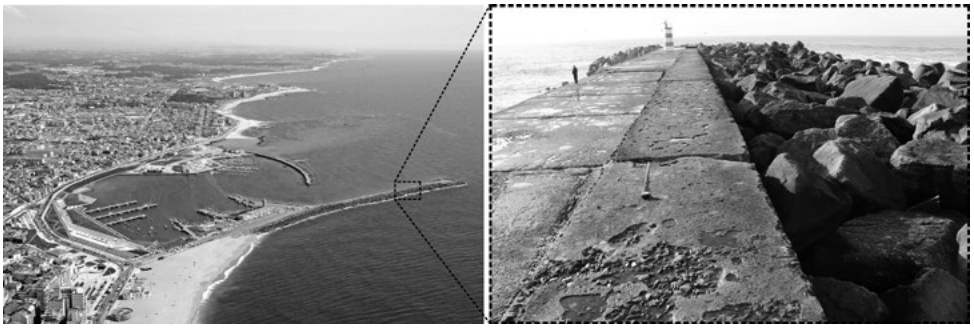

Figure 13: Location of the case study – Póvoa de Varzim Lighthouse Pontoon, Porto, Portugal.

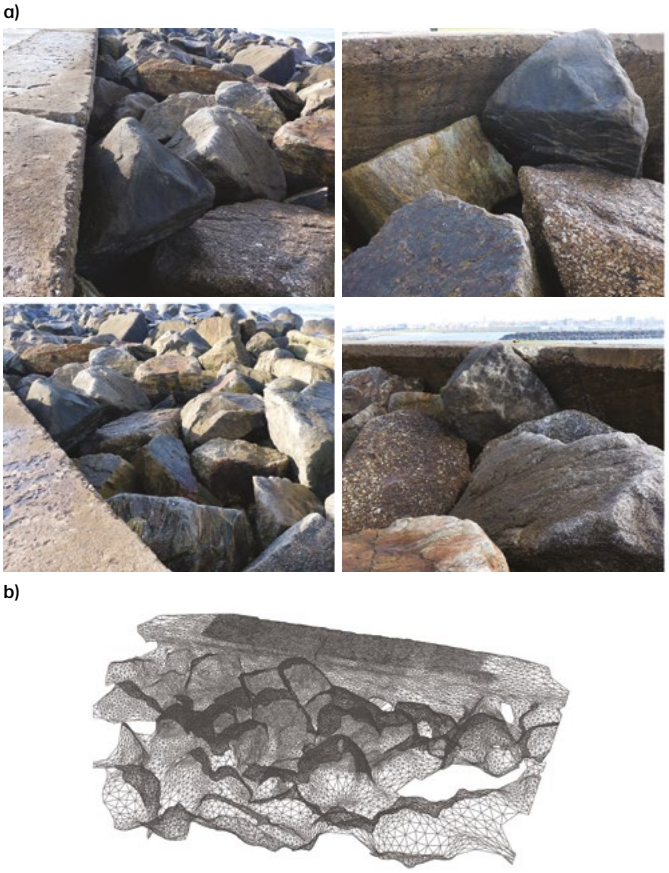

Figure 14: Example of four photos used for local photogrammetry (a) and the generated mesh (b).

Figure 16: 3D simulation of the designed platform, highlighting the section to be produced.

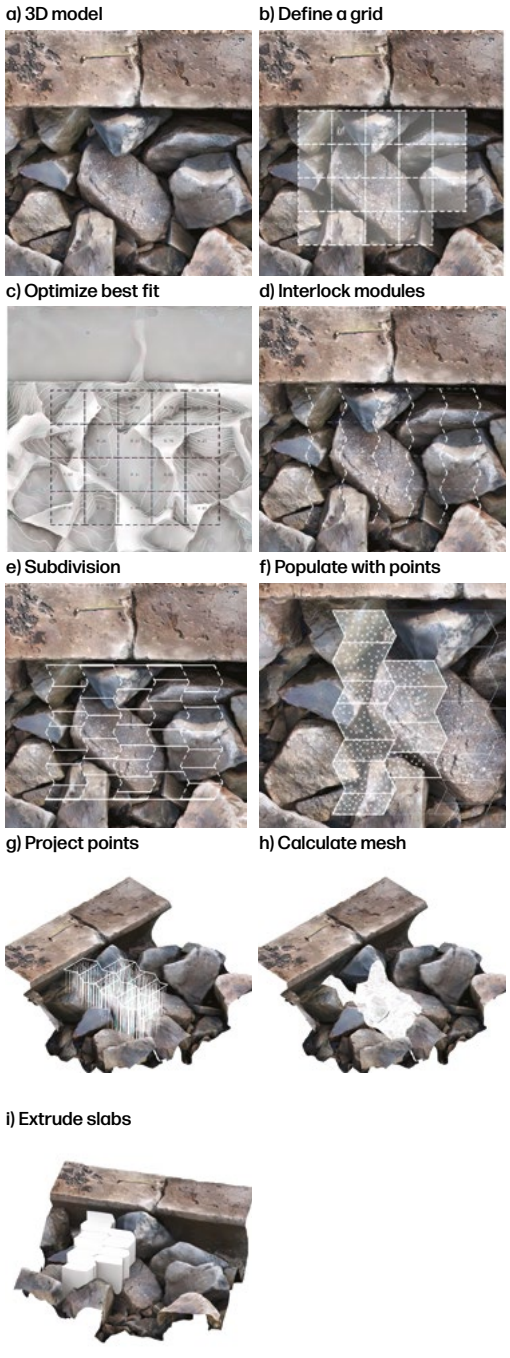

Figure 15: Generative scheme of a platform.

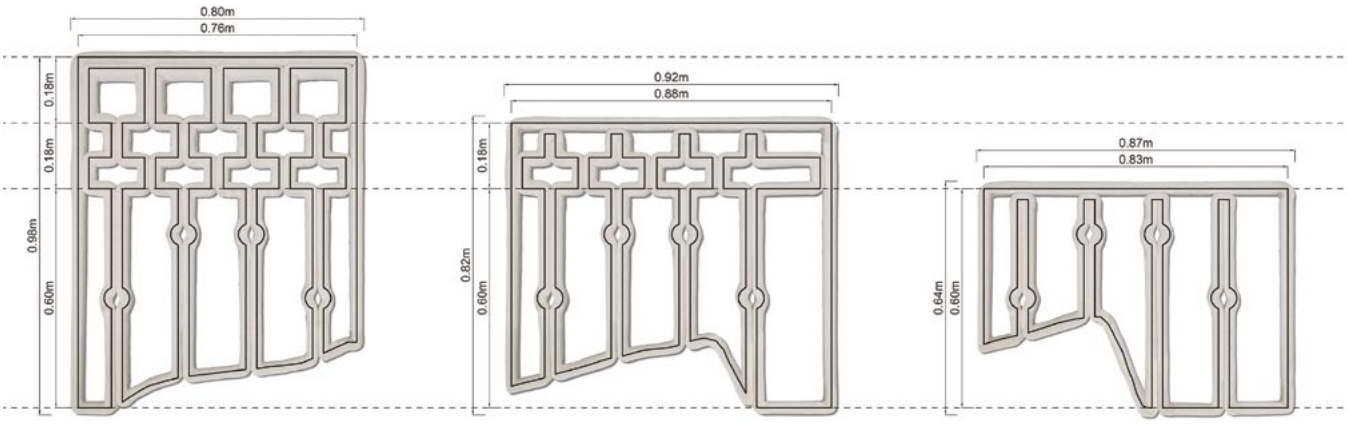

Figure 17: Different infill strategies to reinforce printed components and support upper layers.

Figure 18: Exploded view of the different sections of the printed modules.

Figure 19: Printing process of a full-scale prototype (a) and post-tensioned assembly of two printed sections (b).

Figure 20: Milling process of the cork base.

Figure 21: Artificial topography in cork produced through laboratory milling.

Figure 22: Fully assembled prototype in the ARENA Laboratory after post-tensioning application.

Scan-to-3Dprint methodology to enable site-specific adaptations. Additionally, the system was designed following DfAD principles, ensuring modularity, reusability, and long-term adaptability.

The final prototype successfully demonstrated full structural functionality without requiring chemical bonding between components, allowing for assembly and disassembly without causing damage to the structure or its surrounding environment. Due to its modular nature, individual components can be easily replaced by releasing the post-tensioning system, inserting the new element, and re-applying tension to the steel cables. Ultimately, the components can be reused after disassembly, enabling seasonal deployment and reinstallation year after year. Furthermore, the design avoids mixing different materials, ensuring that at the end of its lifecycle, each part can be ground and recycled as aggregate in new cementitious mixtures. This approach enhances the sustainability of the proposal by promoting circular economy principles.

All prototypes validate the application of 3DCP in architectural and infrastructural systems, reinforcing its role in accelerating construction processes, minimizing material waste, and enabling mass customization. It also suggests that robotic 3DCP prefabrication can contribute to construction efficiency, offering scalable and sustainable alternatives for contemporary architecture and engineering. Future research should further investigate the mechanical performance, durability, and long-term resilience of these printed structures, as well as expand the integration of alternative, low-carbon cementitious materials to enhance environmental sustainability. By continuing to refine these methodologies, 3DCP can play a transformative role in shaping more adaptable, efficient, and sustainable built environments.

ACKNOWLEDGEMENTS

This work is financed by the Project Lab2PT - Landscapes, Heritage and Territory laboratory - UIDB/04509/2020 through FCT - Fundação para a Ciência e a Tecnologia and by FCT Doctoral Grant with the reference SFRH/BD/145832/2019. The work is co-funded by the European Regional Development Fund (ERDF) through the Operational Competitiveness and Internationalization Programme (COMPETE 2020) of the Portugal 2020 Program [Project No. 47108, "SIFA"; Funding Reference: POCI-01-0247-FEDER-047108]. We are grateful to the School of Architecture, Arts and Design of the University of Minho for hosting and supporting the development of the research. We are also grateful to Saint-Gobain Weber for its monitoring and supply of the material.

REFERENCES

[1] B. Kolarevic, "Architecture in the Digital Age, Design and Manufacturing". Oxon: Taylor & Francis. 2005.

[2] T. Boden, B. Andres, G. Marland, "Global CO 2 Emissions from Fossil-Fuel Burning, Cement Manufacture, and Gas Flaring": 1751–2013, Oak Ridge National Laboratory, Oak-Ridge, 2016.

[3] K. L. Scrivener, M. J. Vanderley, and M. G. Ellis. "Eco-Efficient Cements: Potential Economically Viable Solutions for a Low-CO_2 Cement-Based Materials Industry." In *Cement and Concrete Research* 114, 2018, 2–26. https://doi.org/10.1016/j.cemconres.2018.03.015.

[4] R. A. Buswell, W. R. Leal de Silva, S. Z. Jones, and J. Dirrenberger, "3D printing using concrete extrusion: A roadmap for research" In *Cement and Concrete Research*, vol. 112, pp. 37–49, 2018, DOI:10.1016/j.cemconres.2018.05.006.

[5] ACTech – Additive Construction Technologies. University of Minho. Accessed January 7, 2025. https://actech.uminho.pt/

[6] Durmisevic, E. "Transformable Building structures: Design for disassembly as a way to introduce sustainable engineering to building design & construction", 2006, Delft: Cedris M&CC

[7] K. Ostapska, P. Rüther, A. Loli, K. Gradeci, "Design for Disassembly: A systematic scoping review and analysis of built structures Designed for Disassembly", In *Sustainable Production and Consumption*, Volume 48, 2024, Pp 377-395, ISSN 2352-5509, https://doi.org/10.1016/j.spc.2024.05.014.

[8] J. Ribeiro, B. Figueiredo, P. J. S. Cruz, A. Camões; "Concrete AM: Status of the Development of a Robotic Arm-Based Extrusion Setup", In *AM PERSPECTIVES: Research in additive manufacturing for architecture and construction,* P. Rosendhal, B. Figueiredo, M. Turrin, U. Knaack, P.J.S. Cruz (ed.); Lab2PT, University of Minho; ISM+D, TU Darmstadt; SOAP – Stichting OpenAc-cess Platforms, Rotterdam. 2024. pp. 167-182.

[9] Le, T.T., Austin, S.A., Lim, S., Buswell, R.A., Gibb, A.G.F. & Thorpe, T. "Mix design and fresh properties for high-performance printing concrete". In *Materials and Structures*, 45. 2012. pp. 1221–1232.

[10] B. Zahabizadeh, V.M.C.F. Cunha, J. Pereira & C. Gonçalves. "Development of cement-based mortars for 3D printing through wet extrusion". In *IABSE Symposium 2019 Guimarães - Towards a Resilient Built Environment - Risk and Asset Management*. 2019. pp. 540-547.

[11] W.R.L. da Silva, "3D concrete printing: from material design to extrusion," Presented slides in Annual Civil Engineering Workshop at Ecole Centrale de Lille (ACE Workshop 2017), 2017.

[12] J. Carvalho. 2025. Integração de Processos Digitais no Desenho e Fabrico Aditivo de Sistemas Arquitetónicos Cerâmicos. Doctoral thesis defended at the School of Architecture of the University of Minho.

[13] García-López, V. I. Águeda, "Hydrodynamic behavior of a novel 3D-printed nature-inspired microreactor with a high length-to-surface ratio," *Chemical Engineering Science*, 2023. DOI: 10.1016/j.ces.2023.118245.

[14] L. Grigolato, F. Martelletto, and S. Rosso, "A bioinspired geometric modeling approach based on curve differential growth," in *Proceedings of the International Conference of the International Society for Geometry and Graphics*, Springer, 2023. DOI: 10.1007/978-3-031-58094-9_40.

[15] M. Kázmér and D. Taboroši, "Erosional and depositional textures and structures in coastal karst landscapes," in *Coastal Karst Landforms*, Springer, 2013. DOI: 10.1007/978-94-007-5016-6_2.

[16] T. M. Iliffe and L. S. Kornicker, "Worldwide Diving Discoveries of Living Fossil Animals from the Depths of Anchialine and Marine Caves." In *Proceedings of the Smithsonian Marine Science Symposium*, edited by Michael A. Lang, Lynne M. Krupsky, and William M. Tisdale, 269–280. Washington, DC: Smithsonian Institution, 2009.

[17] C. Lange, L. Ratoi, and D. L. Co, "Reformative Coral Habitats – Rethinking Artificial Reef Structures through a Robotic 3D Clay Printing Method." In *RE: Anthropocene, Design in the Age of Humans – Proceedings of the 25th CAADRIA Conference – Volume 2*, edited by D. Holzer, W. Nakapan, A. Globa, and I. Koh, 463–472. Chulalongkorn University, Bangkok, Thailand, August 5–6, 2020. https://doi.org/10.52842/conf.caadria.2020.2.463.

[18] S. Conel, "Coastal Erosion: Causes, Consequences, and Mitigation Strategies." In *Journal of Marine Science Research & Development* 13: 414, 2023, https://doi.org/10.4172/2155-9910.1000414.

[19] N. Hosseinzadeh, M. Ghiasian, E. Andiroglu, J. Lamere, L. Rhode-Barbarigos, J. Sobczak, K. S. Sealey and P. Suraneni, "Concrete Seawalls: A Review of Load Considerations, Ecological Performance, Durability, and Recent Innovations." In *Ecological Engineering* 178: 106573, 2022. https://doi.org/10.1016/j.ecoleng.2022.106573.

[20] A. Haleem, M. Javaid, R.P. Singh, S. Rab, R. Suman, L. Kumar, I. H. Khan, "Exploring the potential of 3D scanning in Industry 4.0: An overview, In *International Journal of Cognitive Computing in Engineering*, 3, 2022, pp 161-171, https://doi.org/10.1016/j.ijcce.2022.08.003.